Pharmaceutical Research, Vol. 8, No. 11, 1991

Research Article

Role of Paracellular Pathway in Nonelectrolyte Permeation Across Rat Colon Epithelium Enhanced by Sodium Caprate and Sodium Caprylate

Toyohiro Sawada,[1] Takahiro Ogawa,[1] Mikio Tomita,[1] Masahiro Hayashi,[1,2] and Shoji Awazu[1]

Received February 12, 1991; accepted June 6, 1991

The enhancing effects of 0.25% sodium caprate (C10) and sodium caprylate (C8) on the paracellular permeation of seven water-soluble nonelectrolytes (inulin, polyethylene glycol 900, mannitol, erythritol, glycerol, thiourea, and urea) across the isolated rat colonic epithelium were examined using the Ussing-type chamber technique. The paracellular changes were also measured by impedance analysis. In both the presence and the absence of enhancers, the permeation clearances (P_m) for inulin (12–15 Å in molecular radius) to erythritol (3.2 Å) increased linearly with the increase in their free diffusion coefficients (D_{fr}), showing the existence of a paracellular shunt pathway unrestricted to any molecular size. Glycerol (2.9 Å), thiourea (2.6 Å), and urea (2.3 Å) had higher clearances than the expected linear values, showing the existence of a restricted paracellular or transcellular pathway. Both C10 and C8 increased the permeabilities in the two pathways, but C10 was more effective than C8. The increase in the permeabilities via the shunt pathway caused by the enhancers was greater than that via the restricted pathway, and thus, the two-phase pattern in the relationship of P_m and D_{fr} was similar to that in the absence of enhancers. The transcellular permeabilities for urea and thiourea, which were obtained from the efflux experiments, were increased by the enhancers. However, the relative increase caused by C10 was smaller than that of the paracellular-restricted permeabilities. The paracellular changes probably were due to the increase in pore area per unit diffusive path length. A decrease in the resistance of the intercellular junctions involving a simultaneous increase of membrane capacitance was observed in the presence of C10, corresponding to an increase of pore area per unit path length. The effect of C10 on the paracellular permeability was reversible, and the junctional resistance, membrane capacitance, and P_m of mannitol returned to the control level following the removal of C10.

KEY WORDS: paracellular pathway; pore pathway; diffusive permeability; nonelectrolyte; transepithelial impedance; rat colon.

INTRODUCTION

Intestinal drug absorption is thought to occur through the transcellular and paracellular pathways (1,2). We previously examined the enhancing mechanism of sodium salts of medium-chain fatty acids, caprate (C10)[3] and caprylate (C8), on the absorption of poorly absorbable drugs such as cefmetazole in the rat colon (3,4). The enhancement in the transcellular pathway was due to membrane perturbation resulting from the interaction of the enhancers and membrane lipids or protein (4,5). The enhancement in the paracellular pathway was explained by the widening of intercellular space, which was quantified as the equivalent pore radius calculated from water transport on the assumption that it occurs exclusively via the pore route (3).

The equivalent pore radius is obtained as an average physical property of a complex biological membrane, assuming that all the pores are uniform cylinders or that they all have the same radius (6). However, for the rabbit ileum (7), the rat jejunum (8), and the rabbit jejunum (9), two permeation pathways have been reported for water-soluble and low lipophilic molecules. In the present study, we examined the substantial pore pathway of the rat colonic membrane, using paracellularly permeable nonelectrolytes with different molecular sizes according to the report of Steward (10). We have evaluated the changes in the pore pathways by the enhancers, i.e., C10 and C8, quantitatively.

We also used impedance analysis to measure the transepithelial resistance and capacitance of the colonic

[1] Department of Biopharmaceutics, Tokyo College of Pharmacy, 1432-1 Horinouchi, Hachioji, Tokyo 192-03, Japan.

[2] To whom correspondence should be addressed.

[3] Abbreviations used: C10, sodium caprate; C8, sodium caprylate; D_{fr}, free diffusion coefficient; P_m, membrane permeation clearance corrected for unstirred water layer; $P_{m,app}$, P_m uncorrected for unstirred water layer; P_m', membrane permeation clearance restricted to small molecules, corrected for unstirred water layer; $P_{m,app}'$, P_m' uncorrected for unstirred water layer; P_t, maximal transcellular permeation clearance uncorrected for unstirred water layer; K, efflux rate constant; V_i, intracellular volume; V_e, extracellular volume; β, ratio of apical membrane clearance to efflux clearance; $|Z|$, impedance; f, frequency; R_j, resistance of intercellular junctions; R_L, resistance of lateral intercellular spaces; C_M, membrane capacitance; C_A, apical microvilli capacitance; C_{BL}, basolateral membrane capacitance; A_p, total pore area; A_s, virtual area for free diffusion; Δx, diffusive path length; a, permeant radius; r, pore radius; α, ratio of a to r.

0724-8741/91/1100-1365$06.50/0

membrane and discuss the validity of the paracellular changes obtained from the permeation experiment. The membrane changes caused by the enhancers were found to be reversible by impedance analysis. The molecular size- or diffusion coefficient-dependent permeabilities of nonelectrolytes in the absence of enhancer (under the control condition) have been reported previously (11).

MATERIALS AND METHODS

Materials

[^{14}C]Urea, [^{14}C]thiourea, [^{14}C]glycerol, [^{14}C]mannitol, [^{3}H]polyethylene glycol 900 (PEG 900), [^{3}H]inulin, [*carboxyl*-^{14}C]dextran (MW 70,000), and *n*-[^{14}C]butanol were purchased from New England Nuclear (Boston, Mass). [^{14}C]Erythritol was obtained from Amersham (Bucks, England). C10 and C8 were obtained from Tokyo Kasei Kogyo (Tokyo). All other reagents were of analytical grade or better.

Membrane Permeation Experiments

The detailed method followed that of our previous paper (11). Briefly, the colonic mucosa of Wistar male rats (250 ± 20 g), which was stripped of underlying muscle, was mounted as a flat sheet in the Ussing-type chambers (0.75-cm^2 exposed surface area, 11-ml inner volume). For the mucosal and serosal solutions, Ringer solution (pH 6.5, 280 mOsm/kg), which is composed of 1.2 m*M* NaH_2PO_4, 125 m*M* NaCl, 5 m*M* KCl, 1.4 m*M* $CaCl_2$, 10 m*M* $NaHCO_3$, and 2 g/liter D-glucose, was employed. To the mucosal Ringer solutions, tracer amounts (1–3 μCi) of ^{14}C- or ^{3}H-labeled nonelectrolytes were added with or without 0.25% enhancers and the permeation amounts from the mucosal to serosal sides were obtained at 37°C for 60 min. Since the initial concentration of permeant compound in the mucosal side was so high and the mucosal-to-serosal permeated amount was so small, the mucosal concentration can be regarded as constant during the experiment. Thus, the apparent membrane permeation clearance ($P_{m,app}$) of nonelectrolytes per unit surface area of colonic membrane (μl/min/cm^2) was obtained from Eq. (1):

$$P_{m,app} = \text{(permeation rate)/(mucosal concentration kept constant during the experiment)} \quad (1)$$

The $P_{m,app}$ values were corrected for the unstirred water layer by the diffusion-limited transport of *n*-butanol to obtain the real membrane permeation clearance (P_m) as shown previously (3).

Efflux Experiments

To the colonic segment prepared as described above, tracer amounts (1–3 μCi) of [^{14}C]thiourea or [^{14}C]urea were loaded at 37°C for 2 hr in advance. After a preliminary 10-min rinse at 37°C, the segment was further rinsed with the label-free Ringer solution at 37°C to get the efflux amounts every 10 min for 120 min. To examine the enhancing effects, C10 or C8 was added into the media for loading and rinsing. Finally, the wet weight of the tissue segment was determined. The maximal transcellular permeation clearance (P_t) was obtained from Eq. (2), which is given elsewhere (10,11):

$$P_t = \beta \cdot (1 - \beta) \cdot K \cdot V_i \leqq 0.25 \cdot K \cdot V_i \quad (2)$$

where β is the ratio of the apical membrane permeation clearance to efflux clearance, K is the efflux rate constant obtained as a slope of log (efflux rate) versus time curve, and V_i is the intracellular volume described below. A value of 0.25 is the maximum of $\beta \cdot (1 - \beta)$ given algebraically (10,11).

Intracellular Volume

Following the permeation experiment with inulin, the colonic mucosa was weighed and then incubated for 2 hr in 0.5 ml label-free Ringer's solution to extract inulin. The extracellular volume (V_e), inulin space, and V_i were obtained from Eqs. (3) and (4), respectively.

$$V_e = \text{(extracted inulin amount)/(mucosal inulin concentration kept constant during the experiment)} \quad (3)$$

$$V_i = \text{[weight (volume) of tissue segment]} - V_e \quad (4)$$

Assay

The respective 1 ml of serosal solution, rinsed solution for efflux, and extracted inulin solution was mixed with 10 ml scintillator cocktail (Scintisol solution EX-H, Dojin Laboratories, Kumamoto, Japan) and ^{14}C and ^{3}H activities were counted by liquid scintillation counter (Aloka 903, Tokyo). The decrease in the counting efficiency resulting from quenching was automatically corrected by the external standard source.

Electrical Measurement

Impedances were measured by a phase-sensitive detection method using a circuit connected with the Ussing-type chamber, shown in the block diagram in Fig. 1. Sine waves from a signal generator (E-1202, NF Co. Ltd., Kanagawa, Japan) were supplied to the membrane as an input signal through a potentiostat (Potentiostat/Galbanostat HA301, Hokuto Denko, Ltd., Tokyo). The amplitude and phase shift between the input and the output signals from the membrane were detected with a phase-sensitive detector (Model 332A, Fuso Seisakusho, Kanagawa, Japan). A real part and an imaginary part of the voltage signal, V_r and V_i, respectively, and those of the electric current signal, I_r and I_i, respectively, were given with a digital multitester (9100EA, Sanwa

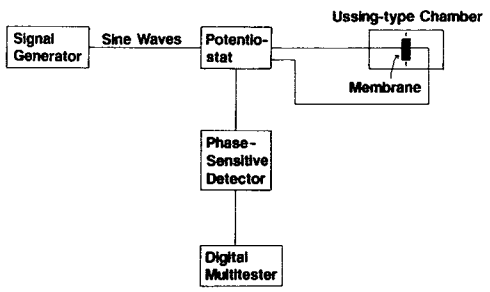

Fig. 1. Block diagram for impedance measurements.

Electric Instrument Co. Ltd., Tokyo), followed by the computation of an admittance (Y) according to Eq. (5):

$$Y = \frac{I_r + j \cdot I_i}{V_r + j \cdot V_i} \quad (5)$$

where j is the imaginary symbol. The impedance ($|Z|$) was obtained as a reciprocal of the admittance. The inner Ag–AgCl electrodes were prepared with silver sheets (3 × 2 cm) as follows: (i) the sheets were cleaned with an emery cloth and defatted with acetone; (ii) they were soaked in 3 M HNO_3 and washed with purified water; and (iii) they were electrolyzed in 0.1 N HCl under an electric current density of 0.4 mA/cm^2. The electrodes were set at the position of 2 mm away from both sides of the membrane. Steady-state impedances at frequencies of 0.015–30 kHz were measured in both the presence of C10 and its absence (control) on the mucosal side. In the Ussing-type chamber without membrane, impedance of the electrode system (electrodes and electrolyte solution) was constant, about 10 Ω · cm^2 at all frequencies and the value was not changed in the presence of C10. Thus, each mucosal epithelium impedance at any frequency was obtained from the observed total impedance minus the electrode electrode impedance. Since the colonic membrane was stripped of underlying muscle, submucosal (sheath) impedance, which was determined by Pappenheimer (13), was neglected.

Impedance Analysis

Steady-state impedances were analyzed according to the simplest one of the distributed resistance models proposed for gall bladder, urinary bladder, or gastric mucosa (12), as shown in Fig. 2. The model was applied to the small intestine by Pappenheimer (13), which is composed of the resistance of the intercellular junctions (R_j) connected with the distributed resistance of lateral intercellular spaces (R_L) in series and with the membrane capacitance (C_M) in parallel. C_M is the lumped capacitance composed of the apical microvilli capacitance (C_A) and the basolateral membrane capacitance (C_{BL}). The capacitances are in proportion to the histological membrane surface areas (13). C_A is much greater than C_{BL} since the surface area of the apical membrane having microvilli structure is much greater than that of the basolateral membrane, indicating that C_{BL} is determined primarily by impedance analysis. The impedance-frequency function is analyzed by the following equation (13):

$$|Z| = \sqrt{\frac{Z_0^2 + \{2 \cdot \pi \cdot f \cdot (Z_0 - Z_\infty) \cdot C_M \cdot Z_\infty \times 10^{-3}\}^2}{1 + \{2 \cdot \pi \cdot f \cdot (Z_0 - Z_\infty) \cdot C_M \times 10^{-3}\}^2}} \quad (6)$$

where f is the frequency (kHz), Z_0 is the $|Z|$ value (Ω) at low frequencies that is equivalent to $R_j + R_L$, and Z_∞ is that at high frequencies that is equivalent to R_L. Z_0, Z_∞, and C_M (μF) were obtained by a nonlinear least-squares fit of the relationship between $|Z|$ and f to Eq. (6) [program MULTI (14)].

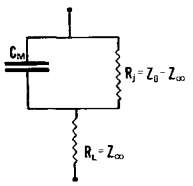

Fig. 2. Distributed model used in the impedance analysis (12,13). R_j is the intercellular junctional resistance; R_L, the distributed resistance of lateral intercellular spaces; C_M, the lumped capacitance expressed by the following equations:

$$1/C_M = (1/C_A) + (1/C_{BL}) \fallingdotseq 1/C_{BL}$$

where C_A is the capacitance of the apical microvilli and C_{BL} is the distributed capacitance of basolateral membrane.

Reversibility of Membrane Changes

To examine the reversibility of the C10 effect on the colonic membrane, the washout groups of C10 were prepared as follows. (i) According to the report of Tomita *et al.* (3,4), the *in situ* loop technique was employed for the treatment of C10. Five milliliters of 0.25% C10 Ringer solution previously warmed to 37°C was added into the colonic lumen (about 8 cm) and allowed to stand for 30 min. The C10 treatment for 30 min *in situ* was previously shown to be effective in the enhancement of the colonic absorption of poorly absorbed drugs such as cefmetazole (3,4). (ii) After the removal of the C10 solution, the lumen was washed out with Ringer solution previously warmed to 37°C at a flow rate of 1 ml/min for 5 min, and thereafter, the lumen was left containing 5 ml of Ringer solution for 5 min. (iii) The lumen was isolated and its mucosa was stripped of underlying muscle, followed by mounting in the Ussing-type chamber as described for the membrane permeation experiment. Finally, the Ringer solution was added to the mucosal and serosal sides and impedance was measured. The mucosal-to-serosal permeation clearance of mannitol was measured after adding mannitol to the mucosal side and corrected for the unstirred water layer. The above group was labeled the washout group. For the control and C10 treatment groups, Ringer solution and 0.25% C10 solution were employed as the solutions in procedures i and iii, respectively.

RESULTS

Alteration in the Paracellular Permeation of Nonelectrolytes in the Presence of C10 or C8

The relationships between the P_m of seven nonelectrolytes corrected for unstirred water layer and their free diffusion coefficients (D_{fr}) are shown in Fig. 3. The results of the control have been previously reported (11). In the presence of C10 or C8, the slopes of P_m vs D_{fr} for inulin, PEG 900, mannitol, and erythritol were increased. The intercept on the ordinate was not significantly different from zero in all cases. The two-phase patterns in Fig. 3 suggest that there are at least two kinds of pores in the paracellular pathways: the large pore (shunt pathway), which is unrestricted by molecular size, and the small pore pathway, which is restricted to molecules smaller than glycerol. Both C10 and C8 enhanced the permeabilities of nonelectrolytes through both pore pathways, and the enhancing effects of C10 were greater than those of C8. In the chamber system employed in this study,

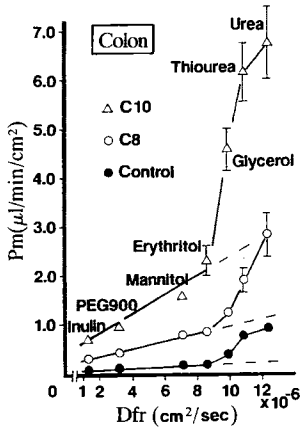

Fig. 3. Effects of 0.25% C8 and C10 on the relationship between the permeation clearances (P_m) of nonelectrolytes across the colonic membrane of rats and their free diffusion coefficients (D_{fr}). Values represent the means ± SE of more than five experiments. The straight lines at the lower diffusion coefficients are analyzed by the linear regression analysis and their correlations are statistically significant in all cases ($P < 0.01$). The regression lines and correlation coefficients are as follows:

$y = 1.07 \cdot 10^4x + 0.0862$ ($r = 0.992$) for the control;

$y = 7.77 \cdot 10^4x + 0.206$ ($r = 0.996$) for C8;

$y = 20.5 \cdot 10^4x + 0.353$ ($r = 0.964$) for C10.

The y-intercepts are not significantly different from zero in any case ($P > 0.05$). The data in the control have previously been reported (11). D_{fr} values are obtained by the relationship $D_{fr} \cdot (\text{molecular weight})^{0.5} = \text{constant}$ (10) and have been listed in a previous paper (11).

the membrane of rat colon is limited to a very small surface area (0.75 cm^2) at both the mucosal and the serosal sides. Therefore, water transport using dextran as a nonabsorbable marker was too small to examine the solvent drag effect.

Enhancing Effects of C10 and C8 on the Shunt and Small Pore Pathways

The slopes (P_m/D_{fr}) in Fig. 3 and the restricted permeation clearances (P_m') of urea and thiourea apparently via the small pore are listed in Table I. P_m' values were obtained by subtracting the extrapolated values on the straight line from P_m in Fig. 1.

P_m/D_{fr} were increased about 7 and 19 times above control values by C8 and C10, respectively. The increases in P_m' for urea and thiourea by C10 were about six times the control ($P < 0.01$). The effect of C8 on P_m' was less than that of C10 and was significant only for urea ($0.05 < P < 0.1$). Thus, the enhancing effects of C10 and C8 on permeability via the shunt pathway were greater than those via the small-pore pathway. The effects of C8 and C10 on the extracellular volume (V_e) obtained as the inulin space also are shown in Table I. The volumes increased about 1.5 and 5 times above control values by C8 and C10, respectively, but these increases are less than those in P_m/D_{fr} values via the shunt pathway.

Contribution of the Transcellular Pathway to the Permeability of Urea and Thiourea

Efflux rates of urea and thiourea from the preloaded colonic membrane in the presence and absence of the promoters are shown in Figs. 4A and B, respectively. The maximal permeation clearances (P_t) of urea and thiourea through the transcellular pathways were calculated by Eq. (2) from the product of the efflux rate constant (K), obtained as the slope in Figs. 4A or B, and the intracellular volume (V_i) obtained by Eq. (4) (Table II).

K values of urea and thiourea were significantly increased by C8 and C10 ($P < 0.01$). P_t values of urea and thiourea are uncorrected for the unstirred water layer and P_m' uncorrected for the unstirred water layer are listed as $P_{m,app}'$ in Table II. Since the unstirred water layers hindering the permeability in efflux (P_t) and mucosal-to-serosal permeability ($P_{m,app}'$) are effectively identical, the ratio of P_t to $P_{m,app}'$ was obtained without correction for the unstirred water layer. The mean of P_t was about 50% that of $P_{m,app}'$ for both urea and thiourea in controls. C10 significantly increased P_t of both compounds ($P < 0.01$), but the increased ratios of P_t were less than those of $P_{m,app}'$, resulting in ratios of P_t to $P_{m,app}'$ for urea and thiourea of about 0.36 and 0.38, respectively. The ratio of P_t to $P_{m,app}'$ in the presence of C8 was reduced to 0.39 only for urea.

Table I. Effects of 0.25% C8 and C10 on Permeability Through the Shunt Pathway, the Apparent Restricted Pore Pathway, and the Extracellular Volume

	P_m/D_{fr}[a] (10^{-4} cm/cm²)	P_m'[b] (μl/min/cm²)		V_e[c] (μl/cm²)
		Urea	Thiourea	
Control[d]	1.07 ± 0.094	0.671 ± 0.020	0.551 ± 0.026	1.18 ± 0.18
C8	7.78 ± 0.50***	1.66 ± 0.42*	0.872 ± 0.250	1.68 ± 0.13**
C10	20.5 ± 4.0***	3.90 ± 0.73***	3.47 ± 0.52***	5.97 ± 0.87***

[a] The slope in Fig. 3. Values are means ± SE of more than five determinations.

[b] The residual P_m obtained by subtracting the extrapolated values on the straight line from P_m in Fig. 3. Values are means ± SE of more than five determinations.

[c] The extracellular space calculated by Eq. (3). Values are means ± SE of six determinations.

[d] Some of the data in the control are shown in a previous paper (11).

* $0.05 < P < 0.10$ vs the control.

** $0.01 < P < 0.05$ vs the control.

*** $P < 0.01$ vs the control.

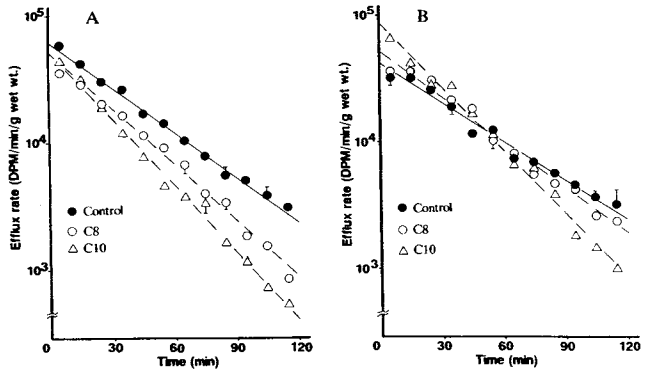

Fig. 4. Effects of 0.25% C8 and C10 on efflux of [^{14}C]urea (A) and [^{14}C]thiourea (B) from the rat colon. Each data point represents the mean ± SE of four experiments. The lines are analyzed by the linear regression analysis and their correlations are statistically significant in all cases ($P < 0.01$). The regression lines and correlation coefficients are as follows:

(A) $y = 7.15 \cdot 10^4 - 0.0269x$ ($r = 0.997$) for the control;
$y = 5.93 \cdot 10^4 - 0.0335x$ ($r = 0.994$) for C8;
$y = 6.43 \cdot 10^4 - 0.0401x$ ($r = 0.996$) for C10;
(B) $y = 4.58 \cdot 10^4 - 0.0232x$ ($r = 0.989$) for the control;
$y = 1.02 \cdot 10^5 - 0.0273x$ ($r = 0.991$) for C8;
$y = 5.82 \cdot 10^4 - 0.0379x$ ($r = 0.994$) for C10.

Effects of C10 on the Resistance of the Intercellular Junctions (R_j), the Distributed Resistance of the Lateral Intercellular Spaces (R_L), and the Membrane Capacitance (C_M)

Figure 5 shows steady-state impedances at frequencies of 0.015–30 kHz in the presence of C10 and in its absence (control) on the mucosal side. C10 sharply decreased impedances at low frequencies. In accordance with Pappenheimer (13), Z_0, Z_∞ (R_L), and C_M (C_{BL}) were obtained by the nonlinear least-squares fit of the data in Fig. 5 to Eq. (6). R_j was calculated as the difference of Z_0 and Z_∞ and is listed together with R_L and C_M in Table III. C10 reduced R_j to about one-seventh the control value and increased C_M to about twice the control. However, significant changes in R_L were not observed.

R_j, R_L, C_M, and P_m of Mannitol After the Removal of C10

R_j, R_L, and C_M obtained by impedance analysis and P_m of mannitol in the washout group of C10 are listed in Table IV together with those in control and C10-treated groups. Comparing the data between the control and the C10-treated groups, the remarkable decrease in R_j and the significant increase in C_M caused by C10 are similar to those in Table III. On the other hand, R_j and C_M in the washout group were not significantly different from those in the control group. The P_m of mannitol in the control and C10-treated groups agreed well with those in the corresponding groups in Fig. 3 and that in the washout group was not significantly different from that in the control group.

DISCUSSION

The relationship between P_m and D_{fr} in Fig. 3 suggests the existence of two paracellular pathways, i.e., the unrestricted shunt pathway available to molecules at least as large as inulin (the large pore) and the restricted pore pathway available to glycerol (radius, 2.9 Å), thiourea (2.6 Å), and urea (2.3 Å) (the small pore). Two such permeation pathways for water-soluble molecules were previously reported in the rabbit ileum (7), rat jejunum (8), rabbit jejunum (9), frog choroid plexus (9) and toad urinary bladder (9). Both 0.25% C10 and C8 increased the P_m of the tested nonelectrolytes, with C10 being more potent than C8 as described previously (3).

For urea and thiourea, the increased permeability ratio via the shunt pathway induced by the enhancers was greater than that via the restricted pore pathway (Table I). The two-phase pattern in P_m versus D_{fr} shows minimal change in the presence of the enhancer. P_m through the pores is expressed by Eq. (7).

$$P_m = (A_p/\Delta x) \cdot (A_s/A_p) \cdot D_{fr} \tag{7}$$

where A_p is the total pore area, Δx the diffusive path length, and A_s the virtual area for the free diffusion. A_s/A_p as expressed by Eq. (8) is obtained from pore theory (15,16):

$$A_s/A_p = (1 - \alpha)^2 \cdot (1 - 2.104\alpha + 2.09\alpha^3 - 0.95\alpha^5) \tag{8}$$

where α is the ratio of the permeant radius (a) to the pore radius (r). The first term on the right side in Eq. (8) defines the steric hindrance at the pore entrance (17); the second term describes the friction of spheres in tubes and was introduced by Renkin into Eq. (8) (16). The permeabilities via the shunt pathway increased linearly with D_{fr} (Fig. 3), indicating that A_s/A_p is constant in Eq. (7), i.e., that α is approximately zero since r is much greater than a. Thus, the increase in P_m induced by the enhancers is due to the increase in $A_p/\Delta x$. The increase in V_e (Table I) is considered to correlate partly with the change in the shunt pathway but further study is necessary to clarify the changes in A_p and Δx in more detail.

In our previous paper (3), the increase in the equivalent pore radius by C10 or C8 was reported using everted sacs. Since the ratio of the water filtration coefficient to water diffusive permeability is used to calculate the radius, $A_p/\Delta x$ and friction cancel out, and only the ratio of steric hindrance is left (6). Thus, the change in A_p and Δx obtained in the present study cannot be evaluated by the equivalent pore concept.

The effluxes of urea and thiourea preloaded in colonic membranes and the effects of C8 and C10 on efflux (Fig. 4) suggest that significant transcellular permeation of urea and thiourea cannot be ruled out in spite of poor lipophilicity. The enhancers also affect the lipoidal membrane as well as the paracellular pathway, as reported previously (4). These results support the suggestion of Wright and Pietras that urea may be, at least in part, permeable in the highly ordered structure of lipids in biological membranes such as in the gall bladder and red blood cells (9).

Impedance analysis has the advantage of yielding both membrane resistance and capacitance, whereas other electrophysiological techniques such as cable analysis and the resistor-variation method yield only resistance (12). Pappenheimer analyzed the relationship between $|Z|$ at steady state

Table II. Effects of 0.25% C8 and C10 on the Permeability of Urea and Thiourea Through the Apparent Restricted Pore Pathway and the Transcellular Pathway

	$P_{m,app}{}'$[a] (μl/min/cm^2)	K[b] (min^{-1})	V_i[c] (μl/cm^2)	P_t[d] (μl/min/cm^2)
Urea				
Control	0.505 ± 0.013	0.0269 ± 0.0001	35.3 ± 2.2	0.238 ± 0.015
C8	0.756 ± 0.158	0.0335 ± 0.0011**	35.1 ± 0.8	0.294 ± 0.007**
C10	0.885 ± 0.102**	0.0401 ± 0.0011**	31.9 ± 1.8	0.320 ± 0.018**
Thiourea				
Control	0.417 ± 0.015	0.0232 ± 0.0011	35.3 ± 2.2	0.205 ± 0.013
C8	0.425 ± 0.117	0.0273 ± 0.0012*	35.1 ± 0.8	0.240 ± 0.005*
C10	0.792 ± 0.087*	0.0379 ± 0.0013**	31.9 ± 1.8	0.302 ± 0.017**

[a] P_m' uncorrected for the unstirred water layer. Values are means ± SE of five determinations.
[b] The efflux rate constant obtained as the slope in Fig. 3. Values are means ± SE of four determinations.
[c] The intracellular volume obtained by Eq. (4). Values are means ± SE of six determinations.
[d] The maximal transcellular permeation clearance calculated by Eq. (2).
* $0.01 < P < 0.05$ vs the control.
** $P < 0.01$ vs the control.

and f in rat small intestine by the simplest distributed model [Fig. 2, Eq. (6)] to examine the change in the paracellular pathway in the presence of glucose or amino acids at a high concentration (13). Although there are other complex models that might fit these data, the simplest model accounted for the paracellular changes. Figure 5 showed similar patterns to Pappenheimer's results and thus, $|Z| - f$ relationships were analyzed by the same model. The R_j value in the control, 61 $\Omega \cdot cm^2$, is greater than that of the small intestine in the presence of glucose as reported by Pappenheimer (13), 14 $\Omega \cdot cm^2$, indicating that the intercellular junction of the colonic membrane is more tight than that of the small intestine. A decrease to about one-seventh of the control for R_j and about a twofold increase for C_M in Table III are results similar to glucose effects on those parameters reported by Pappenheimer (13). If the specific resistance of fluid in the junction, which is reported as 30 $\Omega \cdot$ cm by Schultz and Zalusky (18), is the same as in perfusion fluid (Ringer solution), then $A_p/\Delta x$ (cm/cm^2) in the junction is given as $30/R_j \cdot R_j$ was decreased by C10 to one-seventh of the control value, and thus, $A_p/\Delta x$ was expected to increase about seven times above the control value. However, this ratio of increase is smaller than that obtained from permeabilities in the shunt pathway (19 times) (Table I), suggesting that the decrease in R_j is related to both the shunt pathway and the restricted pore pathway. The twofold increase in C_M approximated that in C_{BL}, suggesting that there is an increase in the surface area of the basolateral membrane. This increase in surface area corresponds with expansion of the lateral intercellular space as enlargement of the paracellular pathway, as shown in electron micrographs (unpublished data). Thus, the decrease in junctional resistance involving a simultaneous increase in capacitance corresponds with the enhancing mechanism of paracellular permeabilities of nonelectrolytes in the presence of the enhancer, C10. Nothing definite can be said about the results in R_L as it is a distributed resistance, which essentially varies with its position along the membrane (12,13).

It is important to examine whether the enhancement in the paracellular permeability by C10 is caused by a reversible change in the epithelium or by irreversible damage. The *in situ* loop technique was employed as an experimental system for the C10 treatment and removal of C10 in this study. The *in situ* system which has an intact blood flow is considered necessary to remove C10 remaining in the epithelium. The changes in R_j, C_M, and P_m of mannitol by C10 obtained *in situ* (Table IV) show a good correspondence with the results in Table III obtained *in vitro*. It was observed that all the above parameters returned to control levels following washout of C10, demonstrating that the C10 effect is reversible. The results in Table IV exclude the possibility that the

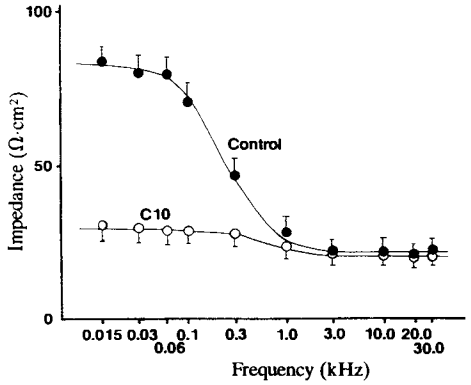

Fig. 5. Steady-state impedances as a function of frequency in the presence of C10 and its absence (control) in the mucosal sides. Values represent the mean ± SE of 10 experiments. The solid lines are best-fit curves calculated using Eq. (6).

Table III. Effects of 0.25% C10 on the Resistance of the Intercellular Junctions (R_j), the Distributed Resistance of Lateral Intercellular Spaces (R_L), and the Lumped Capacitance (C_M)

	R_j ($\Omega \cdot cm^2$)	R_L ($\Omega \cdot cm^2$)	C_M (μF)
Control	61.1 ± 1.1[a]	21.4 ± 0.6	14.7 ± 0.8
+ C10	9.0 ± 0.5	20.2 ± 0.3	28.5 ± 4.9

[a] Values are the best-fit estimates and their SD obtained by the curve-fitting of the data in Fig. 5 to Eq. (6).

Table IV. Reversibility of C10 Effect on the Resistance of the Intercellular Junctions (R_j), the Distributed Resistance of Lateral Intercellular Spaces (R_L), the Lumped Capacitance (C_M), and the Membrane Permeation Clearance (P_m) of Mannitol

Group	R_j[a] ($\Omega \cdot cm^2$)	R_L[a] ($\Omega \cdot cm^2$)	C_M[a] (μF)	P_m[b] ($\mu l/min/cm^2$)
Control[c]	66.7 ± 4.4	14.6 ± 1.8	29.9 ± 3.9	0.134 ± 0.014
C10 treatment[d]	2.1 ± 0.2**	16.9 ± 0.5	43.0 ± 2.6*	1.525 ± 0.065**
Washout[e]	70.5 ± 4.8	13.7 ± 1.2	26.6 ± 4.7	0.107 ± 0.008

[a] Mean ± SE of five or six determinations.
[b] Mean ± SE of six determinations.
[c] Not treated by C10.
[d] The same C10 solution was used also as the washout solution following the C10 treatment.
[e] Prepared by removing C10 with Ringer solution following the C10 treatment.
* $0.01 < P < 0.05$ vs the control group.
** $P < 0.01$ vs the control group.

surface activity of C10 induces irreversible membrane damage. It was also determined that C10 did not enhance water-soluble nonelectrolyte permeability in the jejunal membrane (unpublished data) and that the C10 effect is specific for colonic membrane. This adds supporting evidence to exclude irreversible membrane damage by surface activity of C10.

In summary, although the changes in the pore size for the two paracellular pathways were not fully quantitated, changes in A_p and Δx obtained in the present study provide effective information regarding the mechanism of permeation of poorly absorbable drugs through the paracellular pathway.

ACKNOWLEDGMENTS

This work was supported by a Grant-in-Aid for Scientific Research provided by the Ministry of Education, Science and Culture of Japan (No. 63571101). The authors are very grateful to Dr. Fumiyo Kusu and Mr. Koichi Yuasa, Department of Analytical Chemistry, Tokyo College of Pharmacy, for their helpful advice on impedance measurement. The authors also thank Misses Yuko Tanaka and Madoka Chida and Messrs. Jiro Kajita and Kaname Hasegawa for their technical assistance.

REFERENCES

1. S. G. Schultz, R. A. Frizzell, and H. N. Nellans. Ion transport by mammalian small intestine. In J. Comroe, I. Edelman, and R. Sonnenschein (eds.), *Annual Review of Physiology*, Annual Reviews, Palo Alto, Calif., 1974, pp. 51–91.
2. D. W. Powell. Barrier function of epithelia. *Am. J. Physiol.* 241:G275–G288 (1981).
3. M. Tomita, M. Shiga, M. Hayashi, and S. Awazu. Enhancement of colonic drug absorption by the paracellular permeation route. *Pharm. Res.* 5:341–346 (1988).
4. M. Tomita, M. Hayashi, T. Horie, T. Ishizawa, and S. Awazu. Enhancement of colonic drug absorption by the transcellular permeation route. *Pharm. Res.* 5:786–789 (1988).
5. H. Kajii, T. Horie, M. Hayashi, and S. Awazu. Fluorescence study of the membrane-perturbing action of sodium caprylate as related to promotion of drug absorption. *J. Pharm. Sci.* 77:390–392 (1988).
6. A. K. Solomon. Characterization of biological membrane by equivalent pores. *J. Gen. Physiol.* 51:335s–364s (1968).
7. R. J. Naftalin and S. Tripathi. The roles of paracellular and transcellular pathways and submucosal space in isotonic water absorption by rabbit ileum. *J. Physiol.* 370:409–432 (1986).
8. I. Hamilton, J. Rothwell, D. Archer, and A. T. R. Axon. Permeability of the rat small intestine to carbohydrate probe molecules. *Clin. Sci.* 73:189–196 (1987).
9. E. M. Wright and R. J. Pietras. Routes of nonelectrolyte permeation across epithelial membranes. *J. Membrane Biol.* 17:293–312 (1974).
10. M. C. Steward. Paracellular non-electrolyte permeation during fluid transport across rabbit gall-bladder epithelium. *J. Physiol.* 322:419–439 (1984).
11. T. Sawada, M. Tomita, M. Hayashi, and S. Awazu. Paracellular channel characterized by non-electrolyte permeation through the colonic membrane of the rat. *J. Pharmacobio-Dyn.* 12:634–639 (1989).
12. J. M. Diamond and T. E. Machen. Impedance analysis in epithelia and the problem of gastric acid secretion. *J. Membrane Biol.* 72:17–41 (1983).
13. J. R. Pappenheimer. Physiological regulation of transepithelial impedance in the intestinal mucosa of rat and hamsters. *J. Membrane Biol.* 100:123–136 (1987).
14. K. Yamaoka, Y. Tanigawara, T. Nakagawa, and T. Uno. A pharmacokinetic analysis program (MULTI) for microcomputer. *J. Pharmacobio-Dyn.* 4:879–885 (1981).
15. F.-R. E. Curry. Mechanics and thermodynamics of transcapillary exchange. In E. M. Renkin and C. C. Michel (eds.), *Handbook of Physiology, Section 2, The Cardiovascular System, Vol. IV, Microcirculation*, American Physiological Society, Bethesda, Md., 1984, pp. 309–374.
16. E. M. Renkin. Filtration, diffusion, and molecular sieving through porous cellulose membranes. *J. Gen. Physiol.* 38:225–243 (1955).
17. J. R. Pappenheimer, E. M. Renkin, and L. M. Borrero. Filtration, diffusion and molecular sieving through peripheral capillary membranes. *Am. J. Physiol.* 167:13–46 (1951).
18. S. G. Schultz and R. Zalusky. Ion transport in isolated rabbit ileum. I. Short-circuit current and Na fluxes. *J. Gen. Physiol.* 47:567–584 (1964).